Shell Effects on Rotational Damping in Superdeformed Nuclei

K. Yoshida and M. Matsuo†

Research Center for Nuclear Physics (RCNP), Ibaraki, Osaka 567-0047, Japan
† *Yukawa Institute for Theoretical Physics , Kyoto University,Kyoto 606-8502, Japan*

§ 1. Introduction

Recent progress in γ-ray spectroscopy has enabled us to study off-yrast levels and associated E2 transitions in rapidly rotating nuclei. The observed rotational bands lie near the yrast line and they are well described as quasi-particle or particle-hole excitations in a rotating mean field. On the other hand, excited states which lie at higher intrinsic excitation energy above the yrast line are hardly observed by means of discrete γ-ray spectroscopy not only because individual levels are populated very weakly but also because they do not necessarily form the rotational band structure due to damping of collective rotational motion[1]. Rotational damping is expected because np-nh configurations on rotating mean field are strongly mixed by residual interaction and they respond differently to Coriolis force. If the rotational damping sets in, E2 decay strength from an excited state spreads out over many final states. To describe microscopically this phenomena, we carried out a shell model diagonalization based on rotating mean field and delta residual interaction[2]. From obtained levels and wavefunctions E2 strength functions are analyzed to investigate fragmentation of E2 decays. We discuss damping in superdeformed nuclei with focuses on a shell effect associated with single particle alignments. We reveal that the shell effect affects rotational damping width and onset of damping as well as level density effect does — an effect of shell gap which decreases dramatically the level density of excited many-particle many-hole configurations[3,4].

§ 2. Shell effect in dispersion of rotational frequency and damping width

The difference of response to Coriolis force is expressed in terms of statistical dispersion of rotational frequencies $\Delta\omega$ associated with different np-nh configurations. Rotational damping width depends on $\Delta\omega$ as $\Gamma_{\rm rot} = 4\Delta\omega$ when spreading width Γ_μ due to the configuration mixing of np-nh states is small enough compared with $2\Delta\omega$ and $\Gamma_{\rm rot} = \frac{(2\Delta\omega)^2}{\Gamma_\mu}$ when Γ_μ is large compared with $2\Delta\omega$. Using the grand canonical ensemble the dispersion of rotational frequency is estimated[5] as $(\Delta\omega)^2 = \frac{1}{\mathcal{J}^2}\sum_n i^2 f_n(1-f_n)$ where $\mathcal{J}$ is average dynamic moment of inertia and i_n is single particle alignment for cranked Nilsson s.p. orbit n, and f_n is Fermi-Dirac distribution for n. If we define alignment density $\rho^{(\nu,\pi)}_{\rm align}(e) = \sum_{n\in\nu,\pi} i_n^2 \delta(e-e_n)$, $\Delta\omega$ is expressed as

$$(\Delta\omega)^2 = \frac{T}{\mathcal{J}^2}(\tilde{\rho}^{(\nu)}_{\rm align}(\lambda_\nu) + \tilde{\rho}^{(\pi)}_{\rm align}(\lambda_\pi)) \tag{1}$$

in terms of the smoothed alignment density $\tilde{\rho}^{(\nu,\pi)}_{\rm align}(\lambda) = \frac{1}{T}\sum_n i_n^2 f_n(1-f_n)$ where $\frac{1}{T}f(1-f) = \frac{d}{d\lambda}f$ is regarded as a normalized smoothing function. Temperature T is determined so that

thermal energy agrees with relevant excitation energy. We plot in Fig.1 neutron contribution to $\Delta\omega$, *i.e.*, $\sqrt{\frac{T}{\mathcal{J}^2}\tilde{\rho}^{(\nu)}_{\rm align}(\lambda_\nu)}$ as a function of Fermi energy for the deformation for superdeformed ^{192}Hg ,together with the cranked Nilsson single particle routhian spectrum. Distinct shell oscillation is seen in the figure. The maximum and minimum of the oscillation are associated with aligned high-N intruders and high-Ω orbits,respectively. For example the maximum at $\lambda \sim 46$ MeV is caused by the lowest and most aligned $N = 7$ orbit (7_1) and the second 7_2 orbit (which originate from $j_{15/2}$), and the next peak at $\lambda \sim 51$ MeV corresponds to 8_1 (and 8_2). On the other hand, $\Delta\omega^{(\nu)}$ takes locally minimum value at around $\lambda \sim 49$ MeV, where there exist no highly aligned orbits, but instead present are the oblate orbits with high-Ω value such as $[514]\frac{7}{2}$, $[512]\frac{5}{2}$, $[505]\frac{11}{2}$ which have little alignments ($i_n \approx 0$). A similar situation is found for proton contribution. On the other hand, around the Fermi surface in $A \sim 150$ superdeformed nuclei lie several high-N intruder orbits $\pi 6$ and $\nu 7$. They enhance $\Delta\omega$ for the nuclei compared with smoothed value. Therefore rotational damping width for ^{192}Hg calculated by means of the microscopic calculation is significantly smaller than $A \sim 150$ superdeformed nuclei(Table.1). We also see that there a factor 2 difference between rotational damping width for $A \sim 150$ superdeformed nuclei ^{152}Dy and ^{143}Eu. Above $N = 86$ and $Z = 66$ superdeformed shell gaps lie several high-Ω orbits. These orbits and slightly large deformation make $\Gamma_{\rm rot}$ smaller than ^{143}Eu.

It is noticed that the rotational damping width $\Gamma_{\rm rot} = 30$keV in superdeformed ^{192}Hg is quite small. It suggests possible occurrence of 'ergodic rotational bands' which means rotational band structures formed by compound intrinsic states (the states whose wave functions have strong configuration mixing). The ergodic rotational bands are expected to realize when the rotational damping width is smaller than the level spacing $d = 1/\rho$ of the all levels at fixed I^π, $\Gamma_{\rm rot} < d$, while wavefunctions of the energy levels are compound mixture of basis many-particle many-hole states[6]. In this occasion, a compound state at spin I decays by E2 transition to a single final compound state at $I - 2$, and hence sequence of such E2 tran-

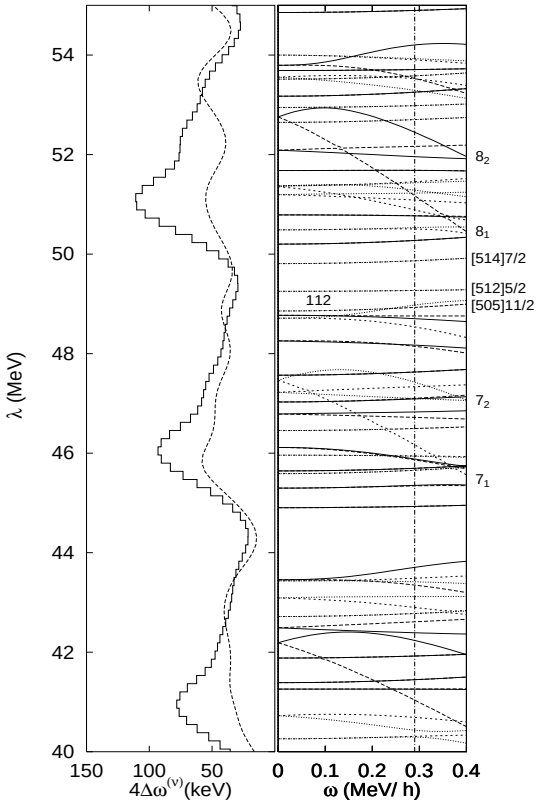

Fig. 1. Neutron contribution to $\Delta\omega$ (alignment density) as functions of Fermi energy λ(solid line) for superdeformed ^{192}Hg. Temperature is taken $T = 0.32$MeV and rotational frequency $\omega = 0.29$(MeV)$/\hbar$ corresponding to $I = 40\hbar$. The diagram also shows some aligned high-N orbits and high-Ω orbits responsible for local maximum and local minimum in the alignment density. Smoothed level density(dashed line) is drawn for comparison.

-sitions forms a band structure in spite of the strong mixing. If ergodic rotational bands are realized, onset of rotational damping should exceeds that of configuration mixing which agrees with the former otherwise as is the case with $A \sim 150$ superdeformed and $A \sim 170$ normally deformed nuclei. Making use of Fermi gas formula for level density, onset energy of configuration mixing is estimated[4] as $E_{\rm onset} \propto A^{-1} a_0^{-5/3}$ assuming that magnitude of residual interaction $\bar{v}$ behaves as $\propto A^{-1}$. Here Fermi gas parameter $a = A/a_0$, and $a_0 = 15, 17$ and 13MeV for ^{143}Eu, ^{152}Dy and ^{192}Hg, respectively. In Table.1 we show onset energy of damping $E_{\rm onset}$ multiplied by a factor $(\frac{A}{192})(\frac{a_0}{13})^{-5/3}$ with which we intend to remove the level density effect. It shows that onset of damping for superdeformed ^{192}Hg is retarded compared with the other nucleus or onset of configuration mixing. It leads to significantly large number of rotational bands $N_{\rm band} \sim 150$ in ^{192}Hg. The microscopic calculation shows that the total level spacing d is ~ 30 keV at $E_x = 1.2$ MeV, and ~ 10 keV at $E_x = 1.6$ MeV for ^{192}Hg. Namely, the rotational damping width is comparable with the level spacing, $\Gamma_{\rm rot} \sim d$, in the energy region under discussion. Thus, the situation lies around the borderline of the condition for the ergodic rotational bands. This suggests that similar mechanism to that of the ergodic rotational bands is taking place in superdeformed ^{192}Hg, and explains why the energy levels in the region of $E_x \sim 1.2 - 1.6$ MeV form rotational band structures and contribute to the large number of $N_{\rm band}$. It should be emphasized that shell effect in single particle alignment plays an important role in the characteristic features of rotational damping in superdeformed ^{192}Hg.

References

1) B. Lauritzen, T. Døssing, and R.A. Broglia, Nucl. Phys. **A457**(1986)61.
2) M. Matsuo, T. Døssing, E. Vigezzi, R.A. Broglia, and K. Yoshida, Nucl. Phys. **A617**(1997)1.
3) S.Åberg, Phys. Rev. Lett. **64**(1990)3119;
   S. Åberg, Prog. Part. Nucl. Phys. vol.28 (Pergamon,1992)p11.
4) K.Yoshida and M. Matsuo, Nucl. Phys. **A612**(1997)26.
5) T. Døssing and B. Herskind, Proc. Intern. Symp. on New Trends in Nuclear Collective Dynamics (Nishinomiya) (Springer-Verlag, 1992)p239
6) B. Mottelson, Nucl. Phys. **A557**(1993)717c.
   S.Aberg, Z.Phys. **A358**(1997)269.

Table I. Calculated rotational damping width $\Gamma_{\rm rot}$, number of rotational bands $N_{\rm band}$ and onset energy of damping $E_{\rm onset}$ for superdeformed nuclei. In the 4th column a factor $(\frac{A}{192})(\frac{a_0}{13})^{-5/3}$ is multiplied to $E_{\rm onset}$ to remove the level density effect.

	$\Gamma_{\rm rot}$(keV)	$N_{\rm bands}$	$E_{\rm onset}$(MeV)	$(\frac{A}{192})(\frac{a_0}{13})^{-5/3} E_{\rm onset}$(MeV)
^{192}Hg	30	150	1.6	1.6
^{152}Dy	50	80	2.5	1.2
^{143}Eu	100	40	2.0	1.2